



Published in final edited form as:

Oncogene. 2015 May 14; 34(20): 2640–2649. doi:10.1038/onc.2014.205.

Actin filament-associated protein 1 is required for cSrc activity and secretory activation in the lactating mammary gland

Jess M Cunnick¹, Stephanie Kim^{2,*}, James Hadsell^{3,*}, Stephen Collins¹, Carmine Cerra⁴, Patti Reiser⁴, Daniel C Flynn⁵, and Youngjin Cho^{1,#}

¹Department of Basic Sciences, The Commonwealth Medical College, Scranton, PA 18509, United States

²Graduate School of Medicine, The Commonwealth Medical College, Scranton, PA 18509, United States

³Fortis Institute Scranton, Scranton, PA18509, United States

⁴Department of Pathology, Pocono Health System, East Stroudsburg, PA 18301, United States

⁵College of Health Science, University of Delaware, Newark, DE 19716, United States

Abstract

Actin filament-associated protein 1 (AFAP1) is an adaptor protein of cSrc that binds to filamentous actin and regulates the activity of this tyrosine kinase to affect changes to the organization of the actin cytoskeleton. In breast and prostate cancer cells, AFAP1 has been shown to regulate cellular responses requiring actin cytoskeletal changes such as adhesion, invadopodia formation and invasion. However, a normal physiological role for AFAP1 has remained elusive. In this study, we generated an AFAP1 knockout mouse model that establishes a novel physiological role for AFAP1 in lactation. Specifically, these animals displayed a defect in lactation that resulted in an inability to efficiently nurse. Histologically, the mammary glands of the lactating knockout mice were distinguished by the accumulation of large cytoplasmic lipid droplets in the alveolar epithelial cells. There was a reduction in lipid synthesis and the expression of lipogenic genes without a corresponding reduction in the production of beta-casein, a milk protein. Furthermore, these defects were associated with histological and biochemical signs of precocious involution. This study also demonstrated that AFAP1 responds to prolactin, a lactogenic hormone, by forming a complex with cSrc and becoming tyrosine phosphorylated. Together, these observations pointed to a defect in secretory activation. Certain characteristics of this phenotype mirrored the defect in secretory activation in the cSrc knockout mouse, but most importantly, the activity of cSrc in the mammary gland was reduced during early lactation in the AFAP1 null mouse and the localization of active cSrc at the apical surface of luminal epithelial

Users may view, print, copy, and download text and data-mine the content in such documents, for the purposes of academic research, subject always to the full Conditions of use:http://www.nature.com/authors/editorial_policies/license.html#terms

*Corresponding Author: Youngjin Cho, PhD, Department of Basic Science, The Commonwealth Medical College, 525 Pine Street, Scranton, PA 18509, United States, Phone: +1-570-687-9171, Fax: 570-504-2808, ycho@tcmedc.org.

[‡]These authors contributed equally

Supplementary information: Supplementary Information accompanies the paper on the *Oncogene* website (<http://www.nature.com/onc>)

Conflict of Interest: The authors declare no conflict of interest.

cells during lactation was selectively lost in the absence of AFAP1. These data define, for the first time, the requirement of AFAP1 for the spatial and temporal regulation of cSrc activity in the normal breast, specifically for milk production.

Keywords

Actin filament associated protein (AFAP); cSrc; prolactin; mammary gland; secretory activation; lactation

Introduction

The known role of the cSrc tyrosine kinase in various cellular functions and cancer progression necessitates a deeper understanding of the adaptor proteins that regulate the spatial and temporal activity of cSrc (1). One such adapter protein, originally identified as a substrate and binding partner of oncogenic variants of cSrc, is the Actin Filament-Associated Protein 1 (AFAP1, formerly AFAP-110) (2). AFAP1 is the prototypical member of a family of three structurally related proteins: AFAP1, AFAP1 like-1 (AFAP1L1), and AFAP1 like-2 (AFAP1L2, alternatively XB-130). The structure of AFAP1 includes two Pleckstrin Homology (PH) domains, one of which harbors a binding site for protein kinase C (PKC) (3), SH2 and SH3 binding motifs for cSrc (4, 5) and carboxy-terminal domains that mediate self-association and interactions with f-actin (6). AFAP1 is a substrate of PKC α as well as the Src family kinases, cSrc and Fyn (2, 4, 7). One proposed function for AFAP1 is that it acts as an adaptor protein that localizes kinases involved in the organization of the actin cytoskeleton (7-10). In addition, AFAP1 can crosslink actin filaments, thereby affecting the integrity of the actin cytoskeleton (3, 6, 11-13).

The function of AFAP1 in oncogenesis has been examined in both breast and prostate cancer. The loss of AFAP1 in prostate cancer cells reduced the rate of proliferation and orthotopic tumor formation in nude mice (14). The loss of AFAP1 also reduced focal complex/adhesion formation and cellular adhesion to extracellular matrix proteins in both breast and prostate cancer cells (10, 14). Silencing of AFAP1 expression in a breast cancer cell line (MDA-MB-231 cells) reduced invadopodia formation (unpublished data) and invasion (15). Although these findings highlight a relevant role for AFAP1 in modulating oncogenesis in the breast and prostate, the normal physiological role of AFAP1 in these tissues has not been determined.

cSrc controls numerous cellular functions such as cytoskeletal remodeling, adhesion, survival and proliferation (16). The increased activation or the overexpression of cSrc leads to dysregulation of these cellular functions and contributes to tumor progression and metastasis in human cancers including breast cancer (17). The physiological functions of cSrc in the breast have been studied by germ line deletion (18-20) and by the conditional deletion of cSrc in mammary epithelium (21). Notably, cSrc null female mice experience lactation failure (20), establishing an important physiological role for cSrc in directing secretory activation.

Secretory activation is a series of molecular and cellular events required for the onset of copious milk production in the mammary gland at parturition. During secretory activation, the expression of specific genes that regulate milk protein and triglyceride synthesis (22-24) as well as secretory activity within mammary epithelial cells are significantly enhanced (22, 25). Secretory activation is regulated by prolactin which also regulates the functional differentiation of the mammary gland during pregnancy in preparation for milk synthesis and secretion (25, 26).

cSrc is a known regulator of the prolactin signaling pathway. In response to prolactin, cSrc binds to the prolactin receptor (PrIR) (27, 28) and is required for the prolactin-induced activation of Signal transducer and activator of transcription 5 (STAT5), a transcription factor downstream of PrIR regulating milk protein expression (29-31). cSrc can also affect the internalization of PrIR (32). Although it is clear that prolactin serves as an input signal to activate cSrc, the exact mechanism of the activation and the regulation of cSrc activity are yet to be addressed.

Considering the prominent role of cSrc in the normal physiology of the breast and the function of AFAP1 as an adaptor and effector of cSrc, we generated a knockout mouse model of AFAP1 to determine the normal physiological function of AFAP1 and to assess its role in lactogenesis and the postnatal development of the mammary gland. Here we report our findings that support the hypothesis that AFAP1 plays an important role in normal breast physiology and is a relevant cSrc adaptor in vivo.

Results

Generation of AFAP1 null mice

To generate AFAP1 knockout (KO) mice, we flanked exon 5 of the *Afap1* gene with LoxP sites (a.k.a. floxed) and mated mice homozygous for the floxed gene with mice expressing Cre under the CMV promoter to produce a heterozygote mouse containing one mutant *Afap1* allele with exon 5 deleted (*Afap1*^{+/-} *exon5*) in every organ. These mice were intercrossed to obtain the AFAP null mice (*Afap1*^{exon5/-} *exon5* or AFAP1^{-/-}). Cre-mediated deletion of exon 5 was designed to introduce a frame shift, generating a stop codon after exon 4. A PCR genotyping strategy was designed to distinguish between the wild type (WT), floxed, and *exon5* allele. Figure 1A shows the location of the primers used for genotyping and the size of the corresponding PCR products in relation to the structure of the indicated alleles. A typical genotyping result is shown in Figure 1B.

AFAP1 knockout (KO) mice were born at the expected Mendelian frequency from the heterozygote intercross with an equal gender ratio and were grossly normal at birth. Western blot analyses with AFAP1 antibodies confirmed the complete absence of AFAP1 protein in murine embryonic fibroblasts (MEFs, see Supplemental Materials and Methods) derived from KO mice (Figure 1C) and in whole mammary glands (Supplementary Figure 3A). AFAP1 protein expression was halved in AFAP1^{+/-} MEFs compared to that in AFAP1^{+/+} MEFs (Figure 1C). There was no compensatory increase or decrease in the expression of AFAP1L2, a closely related AFAP family member, in the KO mammary gland. (Supplementary Figure 3, A and C). Western blotting with antibodies against the amino-

terminus of AFAP1 (F1, (2)) suggested that mRNA consisting of exon 1 through 4 was not expressed as a truncated form of AFAP1 in KO MEFs (data not shown).

Pups born to AFAP1 null dams have a poor survival

Considering the role of cSrc, a known AFAP1 binding protein, in lactation, we examined KO female mice for their ability to nurse. We observed a significant decrease in the 48hr survival rate of all pups born to AFAP1^{-/-} and AFAP1^{+/-} dams compared to that of pups born to the AFAP1^{+/+} dams (Figure 2A). The pups born to KO dams had very small or no milk spots. WT foster dams were able to nurse the pups born to KO dams, whereas KO dams could not foster pups from WT dams (data not shown). We then mated WT females with KO males and KO females with WT males and measured the average weight of all the resulting heterozygote pups daily for 2 weeks. For surviving pups born to KO mice, weight gain was significantly slower if reared by KO dams compared to that of the pups reared by WT dams (Figure 2B). This difference in weight gain was independent of the pup genotype since all the pups were heterozygotes. These data indicated that AFAP1^{-/-} dams were unable to support the survival and growth of their pups due to a deficit in their ability to lactate.

Loss of AFAP1 causes abnormality in lactating mammary glands without affecting the gross development of the mammary gland

To determine the cause of lactation failure in AFAP1^{-/-} mice, we assessed the postnatal development of mammary glands in these mice. Whole mounts of the 4th inguinal mammary glands were prepared at early puberty (4 weeks), sexual maturation (8 weeks), adulthood (14 weeks), late pregnancy (16.5 days post conception, P16.5; the full pregnancy is 18.5 days in C57Bl/B6), and early lactation (3 days postpartum) and analyzed microscopically. No overt differences were observed in mammary glands from virgin mice at 4, 8 and 14 weeks of age and at P16.5 (Figure 3A, a-h). The average length of the main ducts in the WT and the KO mammary glands at full maturation (8 weeks) was similar (Figure 3B). However, whole mounts of lactating mammary glands from AFAP1^{-/-} mice (L3) were significantly less dense with less full alveoli (Figure 3C, k and l) compared to those from AFAP1^{+/+} mice (Figure 3C, i and j).

We compared hematoxylin and eosin (H&E) stained histological sections from mammary glands of AFAP1 WT or null mice at different developmental stages. There were no morphological differences between the mammary glands from WT and KO mice at 4, 8 and 14 weeks in virgin mice (data not shown) and at P16.5 (Figure 4A). In contrast to the WT lactating mammary gland that exhibited expanded large secretory alveoli with milk residue in the lumen (Figure 4B, left panels), KO lactating mammary glands exhibited less expanded alveoli with sparse milk residue in the lumen (Figure 4B, right panels). Furthermore, alveolar epithelial cells from the null lactating mammary glands contained large, clear cytoplasmic droplets (Figure 4B, right panel, arrowhead).

In alveolar epithelial cells, cytoplasmic lipid droplets (CLDs) containing milk fat increase in size and accumulate at the end of pregnancy and decrease immediately after birth as they continuously empty into the lumen with copious milk production (20). The persistence of large CLDs post-partum is indicative of failed secretory activation (22, 25). To confirm the

identity of the enlarged droplets in KO mammary epithelial cells, we immunolabeled mammary gland histological sections with an antibody specific for adipose differentiation related protein (ADRP) that decorates the membrane of CLDs (20, 22). The enlarged droplets within the KO lactating mammary epithelial cells were positively stained for ADRP (Figure 4C, d, white arrow), confirming the intraepithelial retention of large CLDs. In WT epithelial cells in the lactating mammary gland, most of the CLDs aligned closely with the apical surface of the epithelial cells or fused with the plasma membrane as they emptied into the lumen (Figure 4C, c, white arrow head). At P16.5, the size and distribution of CLDs was similar between WT and KO mammary glands (Figure 4C, a and b). These data indicate a possible deficit in secretory activation in the absence of AFAP1.

To ensure that the failure in lactation did not result from a reduced number of mammary epithelial cells constituting each alveolus which would reflect a deficit in cell proliferation during pregnancy, we counted the number of nuclei per alveolus in a captured image of an H&E section of both WT and KO lactating mammary glands. As shown in Supplementary Figure 2, the average cell number of each KO alveolus was comparable to that of WT.

In response to prolactin, AFAP1 becomes tyrosine phosphorylated and forms a complex with cSrc

Secretory activation is regulated by prolactin. To determine the response of AFAP1 to prolactin, we utilized the T47D mammary epithelial cell line known for its high PrlR level (17) and its requirement for cSrc in the prolactin response (27, 33, 34). We expressed GFP-AFAP1 in T47D cells, stimulated the cells with prolactin, and immunoprecipitated GFP-AFAP1. Western blotting indicated that prolactin induced the tyrosine phosphorylation of GFP-AFAP1 (Figure 5A) as well as endogenous AFAP1 (Figure 5B). Furthermore, cSrc co-immunoprecipitated with endogenous AFAP1 upon stimulation of T47D cells with prolactin (Figure 5C). We then tested for the interaction of AFAP1 with cSrc in tissue lysates from mammary glands at P16.5 and L3. AFAP1 co-immunoprecipitated with cSrc from the mammary tissue lysates at L3 but not from those at late pregnancy (Figure 5D). AFAP1 was tyrosine phosphorylated in the tissue lysates from P16.5 and L3 mammary gland (Supplementary Figure 3B). These data demonstrate that AFAP1 binds to cSrc and becomes tyrosine phosphorylated in response to prolactin stimulation.

Since prolactin induces transcriptional changes in multiple genes at secretory activation (22-24), we determined if AFAP1 expression changed. Western blot analysis on mammary gland lysates showed that the AFAP1 protein level remained constant during postnatal development, at P16.5 and at L3 (Supplementary Figure 3A). These data indicate prolactin does not regulate AFAP1 at the level of transcription or translation.

Loss of AFAP1 leads to reduced cSrc activation in early lactating mammary glands

Considering that AFAP1 interacts with cSrc (8, 11, 35), we examined the effect of the loss of AFAP1 on cSrc activity in mammary glands. To measure cSrc activity, we prepared whole tissue lysates from both WT and KO mammary glands from mice at 8 weeks of age, P16.5 and L3. By western blotting, we detected active cSrc using an antibody that recognizes cSrc when it is phosphorylated on tyrosine 418 (pY418) and compared it to the

total level of cSrc. Phosphorylation of this tyrosine is indicative of activation and although this antibody recognizes this phosphotyrosine in all Src family kinases, only cSrc is active during late pregnancy and early lactation (20). In agreement with the previously published work (20), we observed a moderate increase in cSrc activity from P16.5 to L3 in WT mammary glands (Figure 6A). In contrast, the level of active cSrc was drastically reduced in the AFAP1 KO mammary gland at early lactation (Figure 6A). Densitometry of the western blots (n=6 for each genotype) confirmed the reduction of cSrc activity at L3 in the absence of AFAP1 (Figure 6B). Loss of AFAP1 did not affect the level of cSrc expression (Figure 6C).

Next, we visualized the location of active cSrc in the L3 mammary gland with active Src-specific antibody. In the WT mammary gland, strong staining of active cSrc was concentrated on the apical surface and the basolateral sides of luminal epithelial cells and within myoepithelial cells (Figure 6D, a and c, marked with asterisk, arrow and arrowhead respectively). The level of active cSrc was generally decreased in the KO lactating mammary gland (Figure 6D, b and d). Interestingly, the level of active cSrc present at the apical surface of the KO luminal epithelial cells was remarkably reduced compared to WT cells (Figure 6D, b, asterisk), while active cSrc was still detected on the basolateral sides of luminal epithelial cells (Figure 6D, b, arrow) and within myoepithelial cells (Figure 6D, b, arrow head). There was no difference in the location or intensity of total cSrc between WT and KO lactating mammary glands and total cSrc was still present at the apical surface of lactating mammary glands of KO mice (Figure 6E, lower panel, arrow).

We then probed for AFAP1 in histological sections of mouse mammary glands with the F1 antibody. AFAP1 was expressed in luminal and ductal epithelial cells as well as in myoepithelial cells (Supplementary Figure 4A, d, arrow), which matched the AFAP1 expression pattern reported for the human mammary gland (9). There was no increase of AFAP1 detected around the periphery of lipid droplets. We further confirmed the expression of AFAP1 in both luminal epithelial and myoepithelial cells by immunostaining primary mammary epithelial cells cultured on collagen-coated coverslips with the AFAP1 antibody. AFAP1 antibody immunostained both myoepithelial cells (positive for cytokeratin 14, supplementary figure 5A) and luminal epithelial cells (positive for cytokeratin 8/18, supplementary figure 5B). There was no difference in the organization of actin filaments between WT and KO mammary epithelial cells. To precisely determine the subcellular location of AFAP1, we isolated mammary luminal epithelial precursor cells and cultured them into acini in a 3-dimensional culture system (36) and then immunolabeled the acini with anti-AFAP1 antibody. AFAP1 was clearly visible outlining the cellular cortex with equal distribution on the basolateral and apical sides of the cells, exterior to the location of cytokeratin staining (Supplementary Figure 4B). Therefore, the subcellular localization pattern of AFAP1 was identical to that of cSrc. Together, these data indicate that AFAP1 expression co-localizes with active cSrc in the lactating mammary gland, especially at the apical region of luminal epithelial cells, and is required for the normal spatial and temporal activity of cSrc associated with early lactation.

Loss of AFAP1 affects milk lipid synthesis without affecting milk protein synthesis

To identify downstream signaling pathways affected by reduced cSrc activation at secretory activation, we first examined STAT5 activation and milk protein expression. By western blotting with a phosphotyrosine-specific antibody that recognizes the active form of STAT5a and STAT5b, we observed a normal pattern of STAT5 activation in both WT and KO mammary glands including the sharp increase that normally occurs at L3 (Fig 7A and B). Loss of AFAP1 did not affect the level of STAT5 expression at L3 (Figure 7A and C). In immunolabeled histological sections of lactating mammary glands at L3, the intensity and distribution pattern of active STAT5 (Figure 7D, a and b) and total STAT5 (Figure 7D, c and d) were indistinguishable between WT and null mice. Additionally, the loss of AFAP1 did not affect the expression of beta-casein, which is up-regulated at L3 in response to STAT5 activity (22) (Figure 7E). These results indicate that the PlrR to Stat5 signaling axis controlling milk protein synthesis was not altered by the deletion of AFAP1.

During secretory activation and parallel to the PrIR-mediated STAT5 signaling that increases the expression of milk protein, PrIR-mediated sterol regulatory element binding protein 1 (SREBP1) signaling increases the expression of genes required for lipid synthesis such as Acetyl CoA Carboxylase 1 (ACC1) and Fatty Acid Synthase (FAS) (22, 24, 37). In contrast to normal increase in expression of SREBP1 observed in the WT L3 mammary gland during secretory activation, there was reduced expression of SREBP1 in the absence of AFAP1 (Figure 8A, upper panel). Moreover, the loss of AFAP1 led to the reduced expression of ACC1 and FAS (Figure 8A). We then assessed the lipid content of the lactating mammary gland by preparing cryosections of L3 mammary gland and staining them for lipid with Oil Red O. The KO mammary gland showed reduced lipid staining in the lumens of the alveoli and large Oil Red O stained droplets retained within the epithelial cells (Figure 8B). Together, these results indicate AFAP1 is involved in the regulation of milk lipid synthesis, rather than milk protein synthesis, during secretory activation.

KO mammary gland shows signs of precocious involution at early lactation

In the cSrc null lactating mammary gland, the failure of secretory activation led to precocious involution, marked by premature tyrosine phosphorylation of STAT3 (20), a hallmark of mammary gland involution (38, 39). We observed that AFAP1 KO lactating mammary glands displayed a histological sign of involution, the sloughing of mammary epithelial cells into the lumen that exhibited swollen cytoplasm and condensed nuclei (Supplementary Figure 6) even though the dams were nursing pups (40). We then immunolabeled histological sections of L3 mammary glands for tyrosine-phosphorylated STAT3 (active STAT3). The active STAT3 level was markedly elevated in the KO L3 mammary gland (Figure 9A, b), while total STAT3 staining was comparable between WT and KO L3 mammary glands (Figure 9A, c and d). Western blot analysis confirmed the increased activation of STAT3 in the KO lactating mammary gland (Figure 9B).

The nuclear translocation of CAAT Enhanced Binding Protein delta (CEBP δ) is a downstream event of STAT3 activation and another known histological marker of involution (40, 41). We observed nuclear CEBP δ staining only in KO L3 mammary glands (Figure 9C).

These data indicate that the loss of AFAP1 led to molecular and histological signs of precocious involution in the mammary gland that accompanied failed secretory activation.

Discussion

AFAP1 was originally identified in a screen for v-Src substrates (1, 2). The structure of AFAP1 suggests that it functions as an adaptor or scaffolding protein for kinases that regulate the organization of the actin cytoskeleton (8, 42). Although it is known that AFAP1 contributes to prostate carcinogenesis and plays an important role in regulating tumorigenic potential and the adhesion of prostate and breast cancer cells (10, 14), the normal physiological role of AFAP1 has remained unclear. In this first study on the germline ablation of AFAP1 in mice, we have uncovered a physiological role of AFAP1. In the normal mammary gland, AFAP1, as an adaptor of cSrc, regulates secretory activation leading to the onset of milk production.

cSrc activation is spatially coordinated. Inactive cSrc is localized to endosomes in the perinuclear region of cells and activating signals trigger the trafficking of cSrc to the plasma membrane and its concomitant activation (43, 44). The prolactin response in the postpartum mammary gland requires cSrc activity for secretory activation and milk production (20). In the AFAP1 knockout mouse, the loss of AFAP1 in the mammary gland resulted in reduced cSrc activity and led to a failure in secretory activation and milk production. Therefore, this finding is not only consistent with the predicted role of AFAP1 as an adaptor protein of cSrc, but also identifies prolactin as a novel input signal that requires the interaction between AFAP1 and cSrc for downstream signaling. Our data also suggest that the prolactin-induced binding of AFAP1 to cSrc is a required event for the specific apical positioning of active cSrc in the lactating mammary gland. Furthermore, since we did not detect an association of AFAP1 with Jak2 or PrlR or detect prolactin induced serine phosphorylation of AFAP1 by PKC α (unpublished data), we believe that the binding of cSrc to AFAP1, in contrast to other binding partners of AFAP1, is the most relevant in regulating lactation in the mammary gland.

As an adaptor of cSrc, AFAP1 would be expected to mediate only certain functions of cSrc. The germ line ablation of cSrc caused delays in pubertal duct growth due to reduced estrogen receptor α (ER α) signaling (19). In the AFAP1 null mice, the expression level and phosphorylation status of ER α was not affected (unpublished data) and we saw no measurable delay in pubertal duct growth nor did we detect any histological difference in the knockout mammary gland during puberty and pregnancy. Therefore, AFAP1, as an adaptor of cSrc, does not regulate ductal growth under the regulation of estrogen signaling. Consistent with this, delays in pubertal ductal growth were not reported in the conditional knockout of cSrc in mammary epithelial cells (21).

The increase in PrlR expression and Stat5 activation observed at the onset of lactation did not occur in the cSrc null mouse (20). This resulted in reduced milk protein expression (20). Although there was a reduction of cSrc activation in AFAP1 knockout lactating mammary glands, Stat5 activation and milk protein production remained intact. Therefore, AFAP1 does not participate in the PrlR to Stat5 signaling axis. Rather, our work suggests that cSrc

and its interaction with AFAP1 is involved in up-regulation of key proteins in milk lipid synthesis, such as SREBP1 and its downstream targets ACC1 and FAS during secretory activation. A role for cSrc in regulating SREBP1 expression has been reported by others (45, 46), although the precise mechanism by which it occurs has remained elusive. Our work identifies AFAP1 as a novel contributor to the regulation of the lipogenic pathway during milk production and necessitates further examination of cSrc function in lipid biosynthesis during lactation.

CLD accumulation resulting from a defect in CLD secretion can lead to failed lactation and precocious involution (25, 47-49). Interestingly, F-actin is thought to contribute to the contractile machinery regulating CLD secretion (50, 51). Considering that AFAP1 crosslinks F-actin in response to cSrc activation (11-13) and that F-actin participates in CLD secretion, the possibility exists that AFAP1 may act as an effector of cSrc necessary for changes in actin cytoskeletal organization during the emptying of CLDs. In addition, AFAP1 may position cSrc at the apical membrane in proximity with other effector proteins required for the emptying of CLDs into the lumen. Although our analysis of F-actin organization in isolated mammary epithelial cells in 2D did not show any difference between WT and KO cells, the further investigation of the role of AFAP1 and the actin cytoskeleton in the vectorial movement and the positioning of CLDs in 3D will be required to address such possibilities.

In conclusion, our work demonstrates the requirement of an adaptor protein of cSrc, AFAP1, in specifying spatial and temporal activation of cSrc during lactation in mammary gland. AFAP1 appears to act as an effector for specific functions of cSrc, but this does not rule out functional roles for AFAP1 that are not dependent on cSrc activity. The AFAP1 null mice will allow us to uncover other physiological and pathological processes that are regulated by AFAP1 and those dependent on its interaction with cSrc.

Materials and Methods

Generation and genotyping of AFAP1 null mice

AFAP1 floxed mice were generated (Ozgene Pty Ltd, Gentley DC, WA Australia), as described in the supplementary Materials and Methods section. PCR genotyping was performed with the following primers: F1, AACTGGGGTGTCCCTTGAGTG; R1, GCACTGGGGATAAACTTGC; R3, GCAAGTCTCAACACTGCT. The location of the primer and the size of the corresponding PCR products in relation to the structure of different alleles are illustrated in Figure 1A. A Blood and Tissue DNA extraction kit (Qiagen, Valencia, CA) and Platinum Taq® (Life Technologies, Grand Island, NY) was used for DNA isolation and genotyping PCR.

Mice

All mice were maintained on a 12 hr light and dark cycle at the AAALAC approved animal facility in The Commonwealth Medical College. The studies were in accordance with the Guide for the Care and Use of Laboratory Animals (NIH). Unless stated otherwise, female littermates of matching age from heterozygous intercross were utilized.

Survival rate and weight gain

Pup survival was calculated as the percentage of surviving pups in each litter at 48 hr post partum. Weight gain was determined for heterozygote pups born to KO female mice mated with WT males or to WT females mated with KO males. The pups were weighed daily for 2 weeks and average pup weight was calculated by dividing the sum of the whole litter weight by the number of pups in the litter.

Whole mount preparation and histological analysis

The carmine alum stained whole mounts were prepared as described (52). The fourth inguinal mammary gland were fixed in 10% neutral buffered formalin for paraffin embedding and processed for immunohistochemistry as described (9). Oil Red O staining of cryosections of mammary glands was performed as described (53). Stained sections were imaged with a Observer Z1 epifluorescence microscope (Zeiss, Oberkochen, Germany) or with a A1 confocal microscope (Nikon Instruments Inc, Melville, NY).

Antibodies

Antibodies used for immunohistochemistry and western blotting were as follows: Anti-Src (GD11 from BD Bioscience, 36D10 from cell signaling); anti-phosphotyrosine Src (clone 44660G from Life Technologies for immunohistochemistry, catalog # 2101 from cell signaling for western blotting); anti- α SMA (Sigma); anti-cytokeratin 8/18 (Clone5D3, Thermo Fisher); anti-ADFR (Abcam, Cambridge, MA); wheat germ agglutinin (Life Technologies); anti- α casein (Santa Cruz Biotech, Santa Cruz, CA); anti-Stat5 and anti-phospho Stat5 (pY694) (cell signaling); anti-prolactin receptor (H-300 and G-20, Santa Cruz); anti-SREBP1 (Abcam); anti-ACC1 and anti-FAS (Cell Signaling). All fluorescence-labeled secondary antibodies were from Life Technologies.

Morphological analysis

To measure ductal growth, the whole mounts of mammary glands stained with Carmine alum were imaged with a Perfection photoscanner (Epson, Long Beach, CA) or a M2 Bio Stereo microscope (Zeiss). The captured images were imported to NIH Image J software and analyzed as described (54); Lines were drawn along the three longest axis of each mammary gland and the length of the 9 axes were averaged.

Immunoprecipitation and Western blot analysis

The T47D cell line was from ATCC. GFP-AFAP1 (9) or GFP alone were transfected with Fugene HD (Roche, Indianapolis, IN) according to manufacturer's protocol. The transfected cells were starved in serum free medium for 48 hr prior to the stimulation with ovine prolactin (100 ng/ml, Sigma). Lysate preparation and Immunoprecipitation were performed as described (9). Mammary glands were pulverized in liquid nitrogen before solubilized in buffer for immunoprecipitation.

Supplementary Material

Refer to Web version on PubMed Central for supplementary material.

Acknowledgments

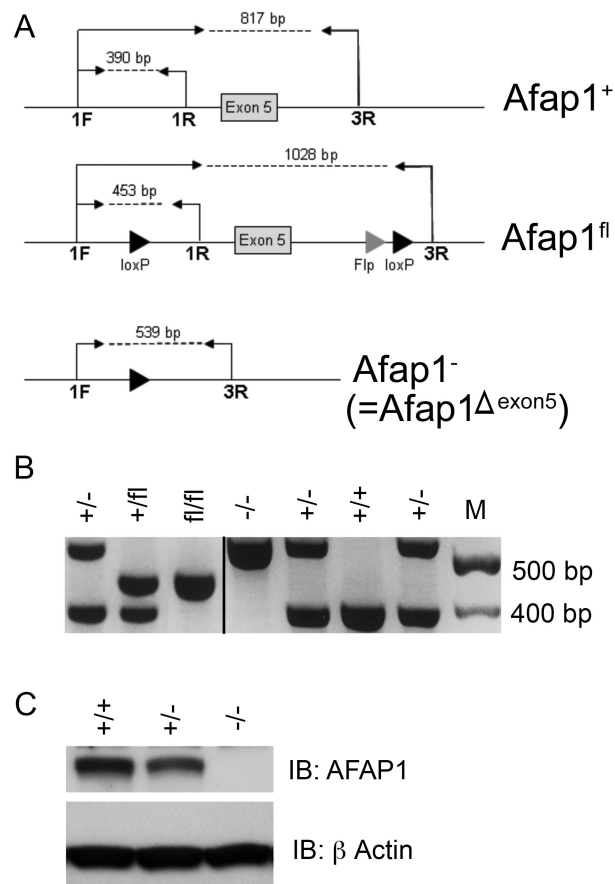
This work is supported by NIH Grant R01CA060731-15A1. We thank Victor Malloy for his care of the mice and Wafa Atamna for cell sorting. We would also like to thank Raj Kumar and John Arnott for the careful reading of our manuscript.

References

1. Reynolds AB, Kanner SB, Bouton AH, Schaller MD, Weed SA, Flynn DC, et al. SRChing for the substrates of Src. *Oncogene*. e-pub ahead of print, Oct 14 2013. 10.1038/onc.2013.416
2. Flynn DC, Leu TH, Reynolds AB, Parsons JT. Identification and sequence analysis of cDNAs encoding a 110-kilodalton actin filament-associated pp60src substrate. *Mol Cell Biol*. 1993; 13(12):7892–900. [PubMed: 8247004]
3. Qian Y, Baisden JM, Cherezova L, Summy JM, Guappone-Koay A, Shi X, et al. PC phosphorylation increases the ability of AFAP-110 to cross-link actin filaments. *Mol Biol Cell*. 2002; 13(7):2311–22. [PubMed: 12134071]
4. Guappone AC, Flynn DC. The integrity of the SH3 binding motif of AFAP-110 is required to facilitate tyrosine phosphorylation by, and stable complex formation with, Src. *Mol Cell Biochem*. 1997; 175(1-2):243–52. [PubMed: 9350057]
5. Guappone AC, Weimer T, Flynn DC. Formation of a stable src-AFAP-110 complex through either an amino-terminal or a carboxy-terminal SH2-binding motif. *Mol Carcinog*. 1998; 22(2):110–9. [PubMed: 9655255]
6. Qian Y, Baisden JM, Zot HG, Van Winkle WB, Flynn DC. The carboxy terminus of AFAP-110 modulates direct interactions with actin filaments and regulates its ability to alter actin filament integrity and induce lamellipodia formation. *Exp Cell Res*. 2000; 255(1):102–13. [PubMed: 10666339]
7. Dorfleutner A, Cho Y, Vincent D, Cunnick J, Lin H, Weed SA, et al. Phosphorylation of AFAP-110 affects podosome lifespan in A7r5 cells. *J Cell Sci*. 2008; 121(Pt 14):2394–405. [PubMed: 18577577]
8. Gatesman A, Walker VG, Baisden JM, Weed SA, Flynn DC. Protein kinase Calpha activates c-Src and induces podosome formation via AFAP-110. *Mol Cell Biol*. 2004; 24(17):7578–97. [PubMed: 15314167]
9. Snyder BN, Cho Y, Qian Y, Coad JE, Flynn DC, Cunnick JM. AFAP1L1 is a novel adaptor protein of the AFAP family that interacts with cortactin and localizes to invadosomes. *Eur J Cell Biol*. 2011; 90(5):376–89. [PubMed: 21333378]
10. Dorfleutner A, Stehlik C, Zhang J, Gallick GE, Flynn DC. AFAP-110 is required for actin stress fiber formation and cell adhesion in MDA-MB-231 breast cancer cells. *J Cell Physiol*. 2007; 213(3):740–9. [PubMed: 17520695]
11. Baisden JM, Gatesman AS, Cherezova L, Jiang BH, Flynn DC. The intrinsic ability of AFAP-110 to alter actin filament integrity is linked with its ability to also activate cellular tyrosine kinases. *Oncogene*. 2001; 20(45):6607–16. [PubMed: 11641786]
12. Baisden JM, Qian Y, Zot HM, Flynn DC. The actin filament-associated protein AFAP-110 is an adaptor protein that modulates changes in actin filament integrity. *Oncogene*. 2001; 20(44):6435–47. [PubMed: 11607843]
13. Qian Y, Baisden JM, Westin EH, Guappone AC, Koay TC, Flynn DC. Src can regulate carboxy terminal interactions with AFAP-110, which influence self-association, cell localization and actin filament integrity. *Oncogene*. 1998; 16(17):2185–95. [PubMed: 9619827]
14. Zhang J, Park SI, Artime MC, Summy JM, Shah AN, Bomser JA, et al. AFAP-110 is overexpressed in prostate cancer and contributes to tumorigenic growth by regulating focal contacts. *J Clin Invest*. 2007; 117(10):2962–73. [PubMed: 17885682]
15. Bourguignon LY, Wong G, Earle CA, Xia W. Interaction of low molecular weight hyaluronan with CD44 and toll-like receptors promotes the actin filament-associated protein 110-actin binding and MyD88-NFkappaB signaling leading to proinflammatory cytokine/chemokine production and breast tumor invasion. *Cytoskeleton (Hoboken)*. 2011; 68(12):671–93. [PubMed: 22031535]

16. Parsons SJ, Parsons JT. Src family kinases, key regulators of signal transduction. *Oncogene*. 2004; 23(48):7906–9. [PubMed: 15489908]
17. Yeatman TJ. A renaissance for SRC. *Nature reviews Cancer*. 2004; 4(6):470–80. [PubMed: 15170449]
18. Shimizu A, Maruyama T, Tamaki K, Uchida H, Asada H, Yoshimura Y. Impairment of decidualization in SRC-deficient mice. *Biol Reprod*. 2005; 73(6):1219–27. [PubMed: 16107610]
19. Kim H, Laing M, Muller W. c-Src-null mice exhibit defects in normal mammary gland development and ERalpha signaling. *Oncogene*. 2005; 24(36):5629–36. [PubMed: 16007215]
20. Watkin H, Richert MM, Lewis A, Terrell K, McManaman JP, Anderson SM. Lactation failure in Src knockout mice is due to impaired secretory activation. *BMC Dev Biol*. 2008; 8:6. [PubMed: 18215306]
21. Marcotte R, Smith HW, Sanguin-Gendreau V, McDonough RV, Muller WJ. Mammary epithelial-specific disruption of c-Src impairs cell cycle progression and tumorigenesis. *Proc Natl Acad Sci U S A*. 2011
22. Anderson SM, Rudolph MC, McManaman JL, Neville MC. Key stages in mammary gland development. Secretory activation in the mammary gland: it's not just about milk protein synthesis! *Breast Cancer Res*. 2007; 9(1):204. [PubMed: 17338830]
23. Naylor MJ, Oakes SR, Gardiner-Garden M, Harris J, Blazek K, Ho TW, et al. Transcriptional changes underlying the secretory activation phase of mammary gland development. *Mol Endocrinol*. 2005; 19(7):1868–83. [PubMed: 15705664]
24. Marcotte R, Smith HW, Sanguin-Gendreau V, McDonough RV, Muller WJ. Mammary epithelial-specific disruption of c-Src impairs cell cycle progression and tumorigenesis. *Proc Natl Acad Sci U S A*. 2012; 109(8):2808–13. [PubMed: 21628573]
25. Palmer CA, Neville MC, Anderson SM, McManaman JL. Analysis of lactation defects in transgenic mice. *J Mammary Gland Biol Neoplasia*. 2006; 11(3-4):269–82. [PubMed: 17136614]
26. Richert MM, Schwertfeger KL, Ryder JW, Anderson SM. An atlas of mouse mammary gland development. *J Mammary Gland Biol Neoplasia*. 2000; 5(2):227–41. [PubMed: 11149575]
27. Acosta JJ, Munoz RM, Gonzalez L, Subtil-Rodriguez A, Dominguez-Caceres MA, Garcia-Martinez JM, et al. Src mediates prolactin-dependent proliferation of T47D and MCF7 cells via the activation of focal adhesion kinase/Erk1/2 and phosphatidylinositol 3-kinase pathways. *Mol Endocrinol*. 2003; 17(11):2268–82. [PubMed: 12907754]
28. Berlanga JJ, Fresno Vara JA, Martin-Perez J, Garcia-Ruiz JP. Prolactin receptor is associated with c-src kinase in rat liver. *Mol Endocrinol*. 1995; 9(11):1461–7. [PubMed: 8584023]
29. Kabotyanski EB, Rosen JM. Signal transduction pathways regulated by prolactin and Src result in different conformations of activated Stat5b. *J Biol Chem*. 2003; 278(19):17218–27. [PubMed: 12621061]
30. Mirmohammadsadegh A, Hassan M, Bardenheuer W, Marini A, Gustrau A, Nambiar S, et al. STAT5 phosphorylation in malignant melanoma is important for survival and is mediated through SRC and JAK1 kinases. *J Invest Dermatol*. 2006; 126(10):2272–80. [PubMed: 16741510]
31. Aksamitiene E, Achanta S, Kolch W, Kholodenko BN, Hoek JB, Kiyatkin A. Prolactin-stimulated activation of ERK1/2 mitogen-activated protein kinases is controlled by PI3-kinase/Rac/PAK signaling pathway in breast cancer cells. *Cell Signal*. 2011; 23(11):1794–805. [PubMed: 21726627]
32. Piazza TM, Lu JC, Carver KC, Schuler LA. SRC family kinases accelerate prolactin receptor internalization, modulating trafficking and signaling in breast cancer cells. *Mol Endocrinol*. 2009; 23(2):202–12. [PubMed: 19056863]
33. Fresno, Vara JA.; Carretero, MV.; Geronimo, H.; Ballmer-Hofer, K.; Martin-Perez, J. Stimulation of c-Src by prolactin is independent of Jak2. *Biochem J*. 2000; 345 Pt 1:17–24. [PubMed: 10600634]
34. Garcia-Martinez JM, Calcabrini A, Gonzalez L, Martin-Forero E, Agullo-Ortuno MT, Simon V, et al. A non-catalytic function of the Src family tyrosine kinases controls prolactin-induced Jak2 signaling. *Cell Signal*. 2010; 22(3):415–26. [PubMed: 19892015]
35. Clump DA, Yu JJ, Cho Y, Gao R, Jett J, Zot H, et al. A Polymorphic Variant of AFAP-110 Enhances cSrc Activity. *Transl Oncol*. 2010; 3(4):276–85. [PubMed: 20689769]

36. Debnath J, Muthuswamy SK, Brugge JS. Morphogenesis and oncogenesis of MCF-10A mammary epithelial acini grown in three-dimensional basement membrane cultures. *Methods*. 2003; 30(3): 256–68. [PubMed: 12798140]
37. Soriano P, Montgomery C, Geske R, Bradley A. Targeted disruption of the c-src proto-oncogene leads to osteopetrosis in mice. *Cell*. 1991; 64(4):693–702. [PubMed: 1997203]
38. Hughes K, Wickenden JA, Allen JE, Watson CJ. Conditional deletion of Stat3 in mammary epithelium impairs the acute phase response and modulates immune cell numbers during post-lactational regression. *J Pathol*. 2011
39. Shackelford TJ, Zhang Q, Tian L, Vu TT, Korapati AL, Baumgartner AM, et al. Stat3 and CCAAT/enhancer binding protein beta (C/EBP-beta) regulate Jab1/CSN5 expression in mammary carcinoma cells. *Breast Cancer Res*. 2011; 13(3):R65. [PubMed: 21689417]
40. Watson CJ, Kreuzaler PA. Remodeling mechanisms of the mammary gland during involution. *The International journal of developmental biology*. 2011; 55(7-9):757–62. [PubMed: 22161832]
41. Thangaraju M, Rudelius M, Bieri B, Raffeld M, Sharan S, Hennighausen L, et al. C/EBPdelta is a crucial regulator of pro-apoptotic gene expression during mammary gland involution. *Development*. 2005; 132(21):4675–85. [PubMed: 16192306]
42. Linder S, Kopp P. Podosomes at a glance. *J Cell Sci*. 2005; 118(Pt 10):2079–82. [PubMed: 15890982]
43. Sandilands E, Brunton VG, Frame MC. The membrane targeting and spatial activation of Src, Yes and Fyn is influenced by palmitoylation and distinct RhoB/RhoD endosome requirements. *J Cell Sci*. 2007; 120(Pt 15):2555–64. [PubMed: 17623777]
44. Sandilands E, Cans C, Fincham VJ, Brunton VG, Mellor H, Prendergast GC, et al. RhoB and actin polymerization coordinate Src activation with endosome-mediated delivery to the membrane. *Developmental cell*. 2004; 7(6):855–69. [PubMed: 15572128]
45. Scott KE, Wheeler FB, Davis AL, Thomas MJ, Ntambi JM, Seals DF, et al. Metabolic regulation of invadopodia and invasion by acetyl-CoA carboxylase 1 and de novo lipogenesis. *PLoS one*. 2012; 7(1):e29761. [PubMed: 22238651]
46. Liu Y, Chen BP, Lu M, Zhu Y, Stemerman MB, Chien S, et al. Shear stress activation of SREBP1 in endothelial cells is mediated by integrins. *Arteriosclerosis, thrombosis, and vascular biology*. 2002; 22(1):76–81.
47. McManaman JL, Palmer CA, Anderson S, Schwertfeger K, Neville MC. Regulation of milk lipid formation and secretion in the mouse mammary gland. *Advances in experimental medicine and biology*. 2004; 554:263–79. [PubMed: 15384582]
48. Ogg SL, Weldon AK, Dobbie L, Smith AJ, Mather IH. Expression of butyrophilin (Btl1a1) in lactating mammary gland is essential for the regulated secretion of milk-lipid droplets. *Proc Natl Acad Sci U S A*. 2004; 101(27):10084–9. [PubMed: 15226505]
49. Vorbach C, Scriven A, Capecchi MR. The housekeeping gene xanthine oxidoreductase is necessary for milk fat droplet enveloping and secretion: gene sharing in the lactating mammary gland. *Genes & development*. 2002; 16(24):3223–35. [PubMed: 12502743]
50. Franke WW, Heid HW, Grund C, Winter S, Freudenstein C, Schmid E, et al. Antibodies to the major insoluble milk fat globule membrane-associated protein: specific location in apical regions of lactating epithelial cells. *The Journal of cell biology*. 1981; 89(3):485–94. [PubMed: 7019216]
51. Amato PA, Loizzi RF. The identification and localization of actin and actin-like filaments in lactating guinea pig mammary gland alveolar cells. *Cell motility*. 1981; 1(3):329–47. [PubMed: 6890874]
52. Dimri M, Naramura M, Duan L, Chen J, Ortega-Cava C, Chen G, et al. Modeling breast cancer-associated c-Src and EGFR overexpression in human MECs: c-Src and EGFR cooperatively promote aberrant three-dimensional acinar structure and invasive behavior. *Cancer research*. 2007; 67(9):4164–72. [PubMed: 17483327]
53. Naylor MJ, Li N, Cheung J, Lowe ET, Lambert E, Marlow R, et al. Ablation of beta1 integrin in mammary epithelium reveals a key role for integrin in glandular morphogenesis and differentiation. *The Journal of cell biology*. 2005; 171(4):717–28. [PubMed: 16301336]
54. Abramoff MD, Magalhaes PJ, Ram SJ. Image Processing with ImageJ. *Biophotonics International*. 2004; 11(7):36–42.

**Figure 1.**

Genotyping and western blot analysis of AFAP1 null mice. A. PCR genotyping strategy. Primers were designed to detect wild type exon 5 of AFAP1 (top), exon 5 flanked by loxP sites (middle) and the Cre-deletion of exon 5 (knockout, bottom) from genomic DNA. B. PCR genotyping results show the 540 bp fragment derived from knockout allele, the 453 bp fragment from the floxed allele, and the 390 bp fragment from the wild type allele. C. Western blot detection of AFAP1 expression from murine embryonic fibroblasts (MEFs) confirms the loss of AFAP1 from AFAP1 null MEFs and shows a 50% reduction of expression in AFAP1^{+/-} MEFs.

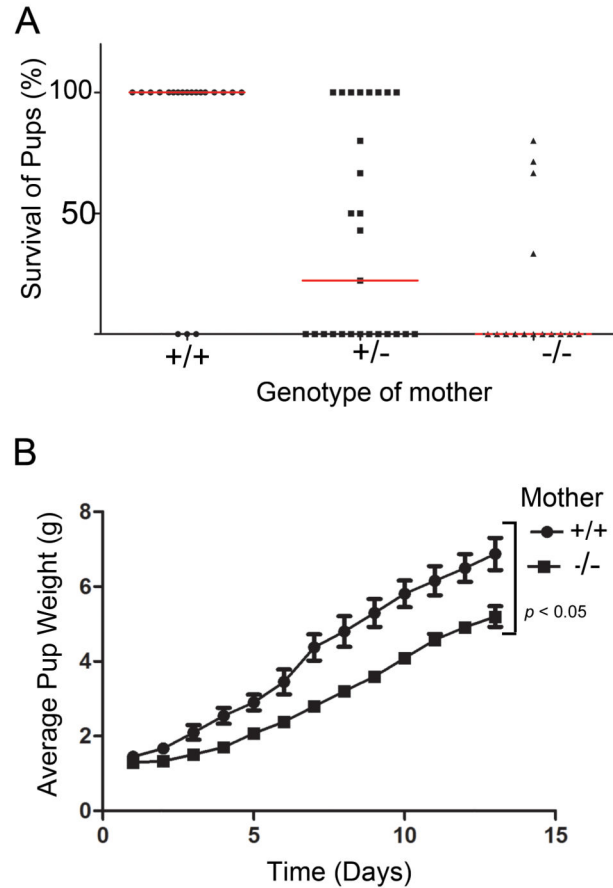


Figure 2.

Survival and weight gain of pups born to AFAP1 null mice are reduced. A. Percent survival of pups within 48 hours after birth nursed by either wild type (circles), heterozygote (squares), or knockout (triangles) dams. Red bars denote the median survival. The difference of the percent pup survival between the wild type dams and knockout dams was statistically significant ($p < 0.01$, one way ANOVA, $N = 27$ pregnancies for wild type; 17 for heterozygote; 17 for knockout). B. Weight gain of heterozygote pups nursed by AFAP1^{-/-} dams compared to the weight gain of heterozygote pups nursed by AFAP1^{+/+} dams. Pups were weighed everyday for 13 days and the average weight of pups in a litter for dams of each genotype ($N=4$ for wild type and $N=3$ for knockout) is presented (mean \pm standard error). The litter size was 9, 8, 5 and 3 for wild type mothers (average 6.3 pups per litter) and 5, 4, and 5 for knockout mothers (average 4.8 pups per litter). The difference in the rate of weight gain was statistically significant ($p < 0.05$, repeated measure ANOVA).

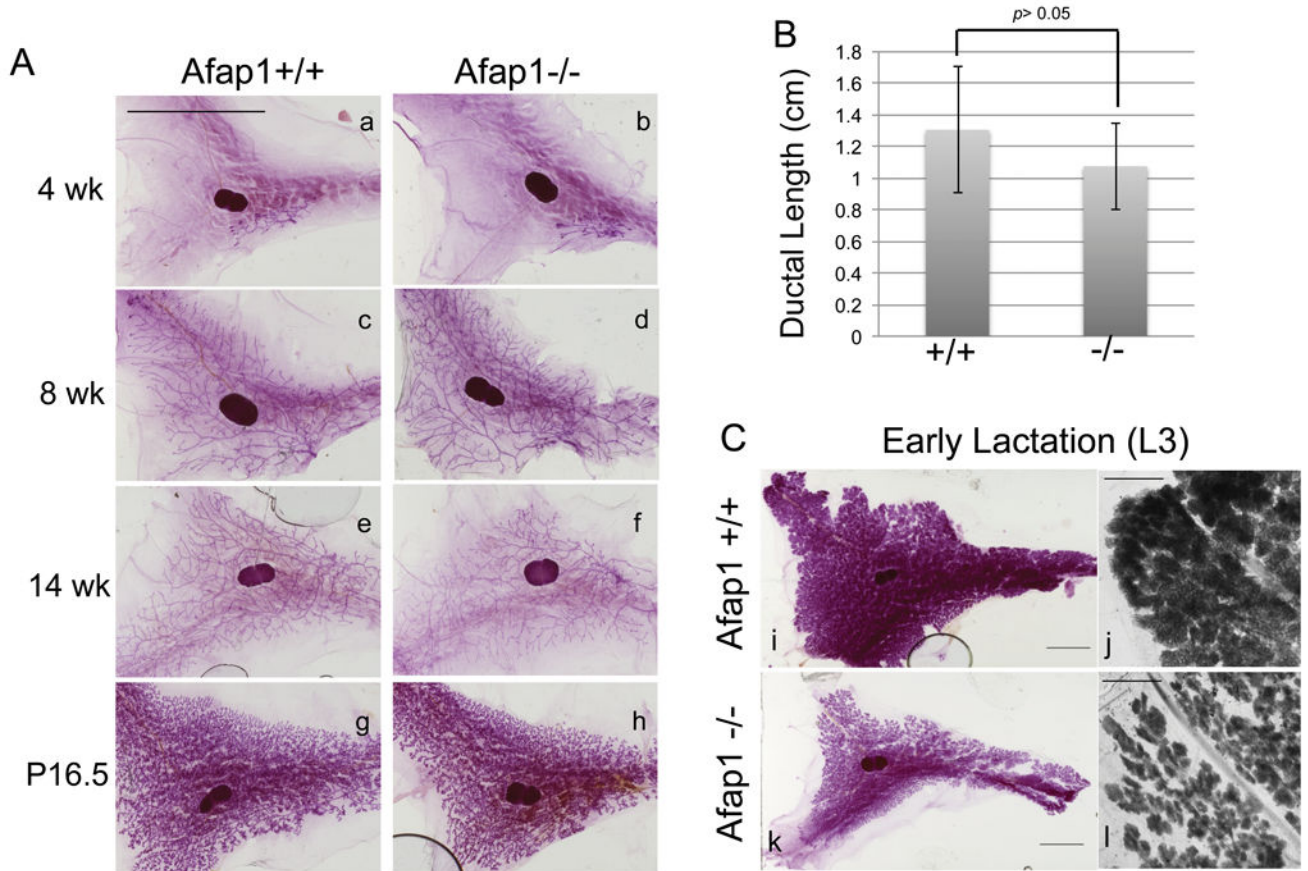


Figure 3.

Mammary glands from lactating AFAP1^{-/-} dams appear abnormal. A. Whole mounts of the fourth inguinal mammary glands at the indicated ages (4 week, 8 week and 14-week-old virgin mice and at pregnancy day 16.5, P16.5) were prepared from AFAP1^{+/+} mice (a,c,e,g) and AFAP1^{-/-} mice (b,d,f,h) and stained with carmine aluminum (Bar = 1 cm). A representative image of three mammary glands per genotype is shown. B. Average ductal length of the fourth inguinal mammary glands from 8-week-old virgin mice. There was no statistically significant difference in ductal length of the wild type and that of the knockout mice, (N=3 each group, $p > 0.05$, t-test, two tailed). C. Whole mounts of the fourth inguinal mammary glands at parturition day 3 (L3) stained with carmine aluminum. The area of attachment to the fat pad was photographed at higher magnification (j, l). (Bars= 5 mm, i and k; 2 mm, j and l)

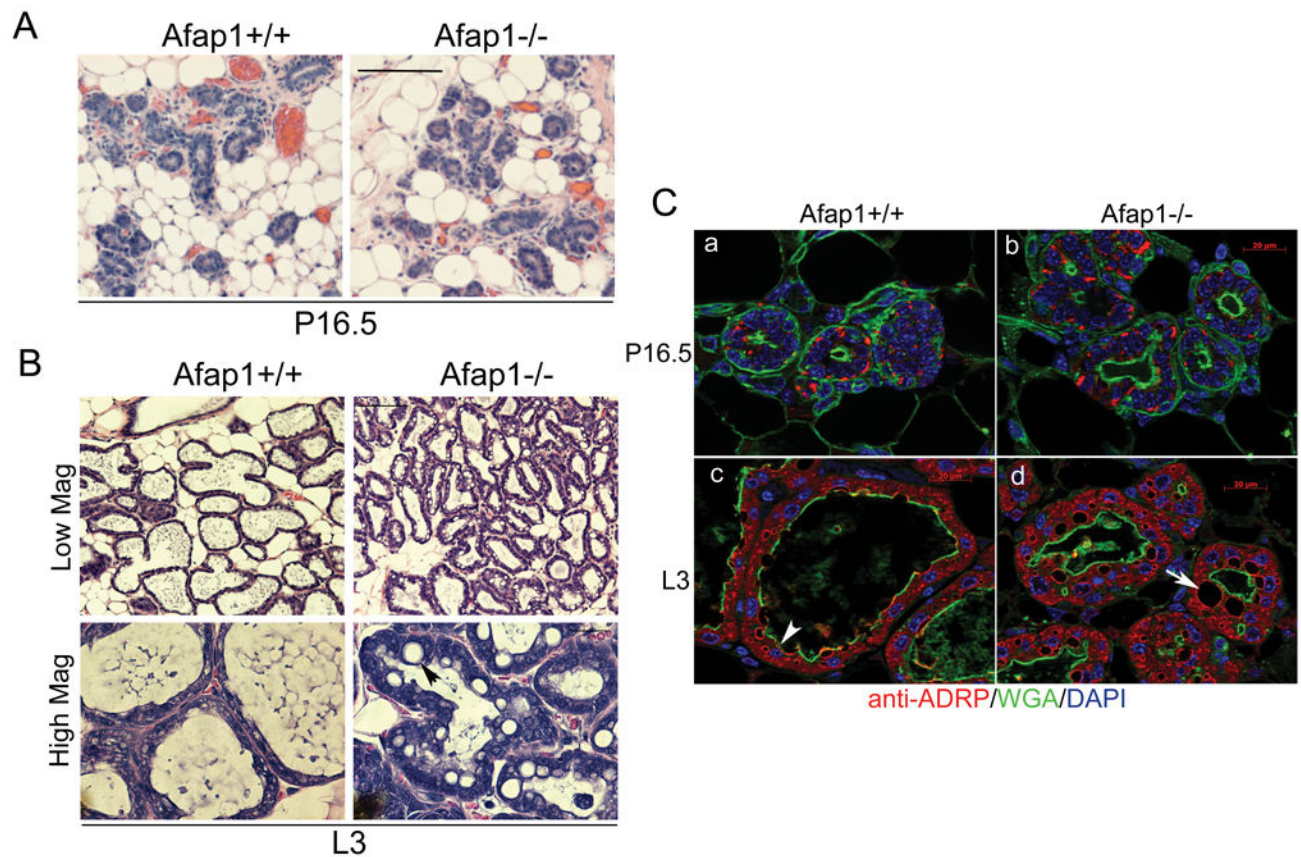


Figure 4.

Large cytoplasmic lipid droplets (CLDs) are persistent post-partum in the AFAP1 null mammary gland. A. Hematoxylin and Eosin (H&E) staining of histological sections of mammary glands at late pregnancy day 16 (P16) (Bar = 100 μm). B. H&E staining of histological sections of mammary glands at lactation day 3 (L3) (Bar = 100 μm, top panels; 20 μm, bottom panel). C. Immunofluorescence staining to identify cytoplasmic lipid droplets (CLDs). Histological sections of mammary glands at late pregnancy (a,b) and lactation day 3 (c,d) were stained with anti-ADRP (Adipose differentiation related protein, alternately known as adipophilin, red) to outline lipid droplets, fluorescence dye conjugated WGA (Wheat germ agglutinin, green) to outline luminal surfaces, and DAPI (blue) to stain nuclei. Normal emptying of CLDs into the lumen of a wild type lactating mammary gland is marked by an arrowhead (c). The retention of large CLDs in the AFAP1 null mammary gland is marked by an arrow (d). Bars = 20 μm (a,b,c,d).

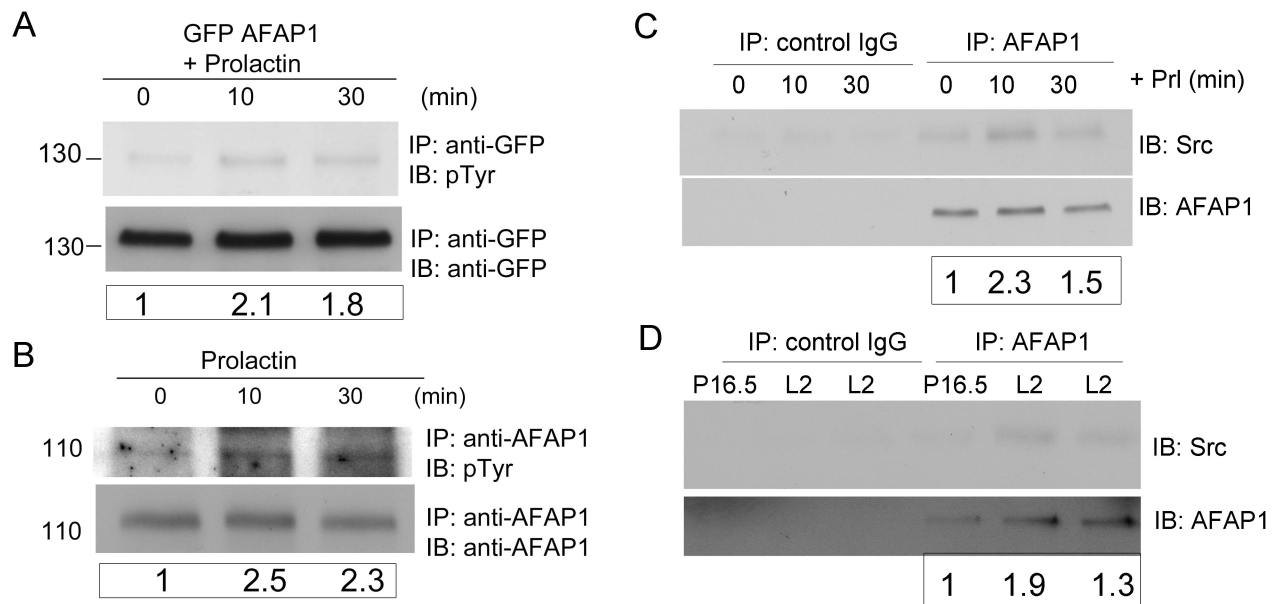
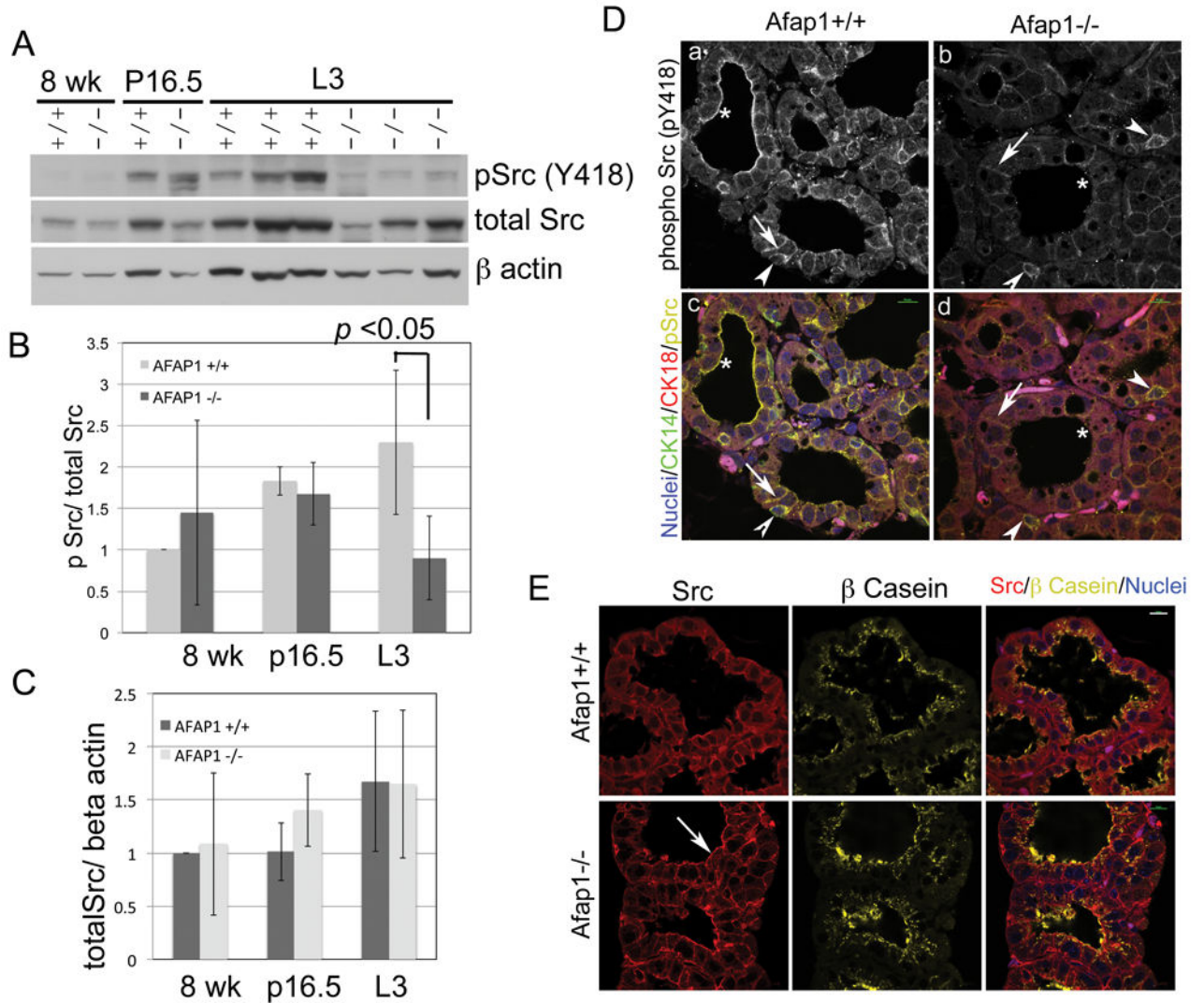


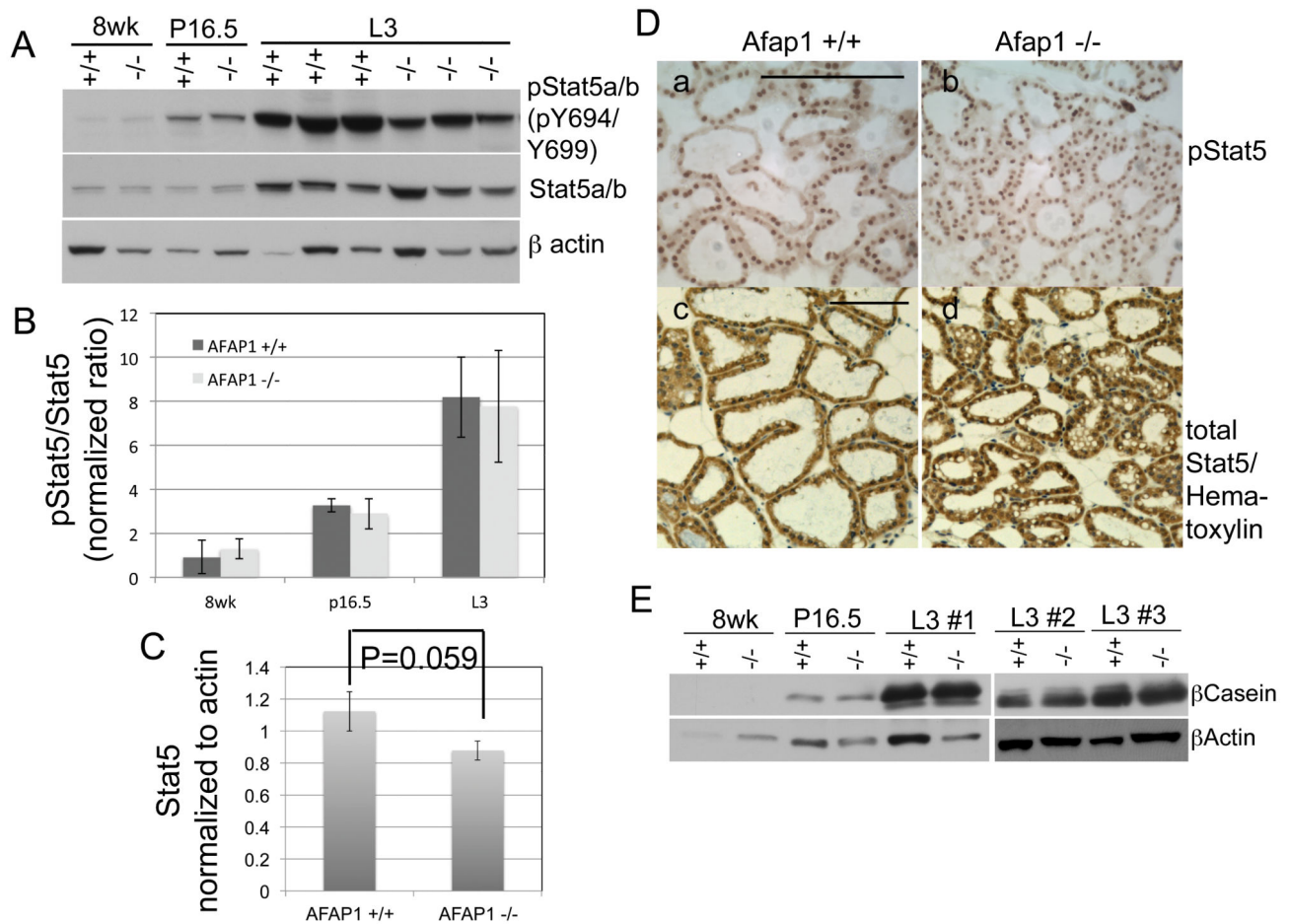
Figure 5.

AFAP1 becomes tyrosine phosphorylated and forms a complex with cSrc in response to prolactin. A. T47D cells expressing GFP-AFAP1 were treated with prolactin. GFP-AFAP1 was immunoprecipitated and immunoblots were probed for phosphotyrosine (top panel) or GFP (bottom panel). The fold-difference in the phosphotyrosine/GFP ratio, compared to that ratio at 0 min, is reported below each lane. B. Endogenous AFAP1 was immunoprecipitated from T47D cells treated with prolactin and immunoblots were probed for phosphotyrosine (top panel) or AFAP1 (bottom panel). The reported fold-differences at the bottom of each lane represent the phosphotyrosine/AFAP1 ratios. C. Lysates of T47D cells treated with prolactin were immunoprecipitated with control IgG or anti-AFAP1 antibody and western blot analysis was used to detect cSrc (top panel) or AFAP1 (bottom panel). The fold-differences reported below the AFAP1 IP lanes represent the Src/AFAP1 ratios. D. Immunoprecipitation with control IgG or anti-AFAP1 antibody was performed on whole mammary gland lysates prepared at late pregnancy (P16) or early lactation (L2), followed by western blot analysis to detect cSrc (top panel), AFAP1 (bottom panel). The fold-differences at L2 represent the Src/AFAP1 ratio for each lane normalized to P16.5. Each western blot in this figure is representative of three independent experiments.

**Figure 6.**

Loss of AFAP1 leads to reduced Src activity in early lactating mammary glands. A. Western blot analysis of tissue lysates prepared from mammary glands of AFAP1 ^{+/+} and AFAP1 ^{-/-} mice at 8 weeks of age, late pregnancy (P16.5) and early lactation (L3). cSrc activation in those tissue lysates was assessed with an antibody specific for active cSrc (pSrc (Y418), top panel). Antibodies that recognize total cSrc (middle panel) and β-actin (bottom panel) were also used. B. Graphical representation of active Src levels normalized to cSrc expression from four different western blots (including the blot in panel A). Densitometry scans of bands representing either active pSrc (Y418) or total cSrc were quantified using ImageJ and the average ratio of pSrc (Y418) to total cSrc levels in the indicated lysates were graphed (bars = standard deviation, n = 6 at L3 for both wild type and knockout lysates). The ratio of pSrc/total Src of all the samples was normalized to that of wild type at 8 weeks. The differences in active Src levels were statistically significant ($p < 0.05$, two-tailed t-test) for the L3 lysates. C. An analysis similar to that described for the graph in B was used to determine the ratio of total cSrc to β-actin in lysates from mammary glands at the indicated times (bars

= standard deviation, n = 6 at L3 for both wild type and knockout lysates). D. Histological sections of mammary glands from wild type and knockout mice at lactation day 3 were stained with anti-active Src[phosphoSrc (Y418)] antibody (white in a and b, yellow in c and d), cytokeratin14 (CK14, green) for myoepithelial cells, cytokeratin 8/18 (CK8/18, red) for luminal epithelial cells and DAPI (nuclei, blue). Image a and b show anti-active Src staining only. Merged images appear in c and d. Arrows mark examples of active Src staining on the basolateral side of luminal epithelial cells. Arrowheads mark examples of the active cSrc in myoepithelial cells. Asterisks mark examples of active Src staining on the apical side of luminal epithelial cells. Note the specific reduction in active Src signaling on the apical side of luminal epithelial cells in the KO L3 gland (asterisk, b and d) E. Histological sections from wild type and knockout mammary glands at L3 were stained with anti-cSrc (red), β -casein (yellow) and with DAPI (blue, nuclei). The arrow marks an example of total cSrc staining on the apical side of luminal epithelia cells in the KO gland.

**Figure 7.**

Tyrosine phosphorylation of STAT5 and β -casein expression are not affected by the loss of AFAP1 during early lactation. A. Tissue lysates were prepared from the mammary glands of AFAP1 +/+ and AFAP1 -/- mice at 8 weeks of age, late pregnancy (P16.5) and early lactation (L3). STAT5 activation was assessed from those tissue lysates by western blotting with antibodies specific for active STAT5a and STAT5b [phosphoSTAT5a/b (Y694/Y699) respectively, top panel] or total STAT5a and STAT5b (middle panel). STAT5a and STAT5b are collectively marked as STAT5 here in. The bottom panel is of the same western blot probed with an antibody specific for β -actin. B. Graphical representation of the average of the ratios of active phosphoSTAT5 to total STAT5 for each lysate (bars = standard deviation, n=3 at 8 wk and P16.5 for both wild type and knockout lysates, n = 6 at L3 for both wild type and knockout lysates). C. A graphical representation of total STAT5 normalized to β -actin in lysates prepared from mammary glands from mice at L3 (bars = standard deviation, n=6). D. Histological sections of mammary glands at early lactation (L3) were prepared from AFAP1 +/+ and AFAP1 -/- mice and stained for phosphoSTAT5 (a,b, bars = 200 μ m) and total STAT5 together with hematoxylin counterstaining (c,d, bars = 100 μ m). E. As in A, mammary gland tissue lysates were prepared at different time points and

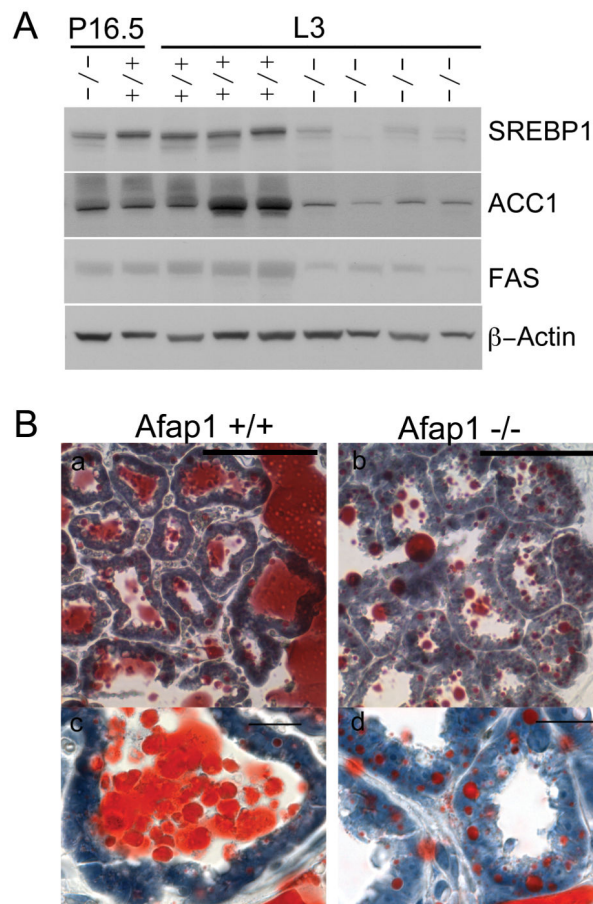
analyzed for milk protein expression (β -casein, top panels). β -actin expression was used as a loading control.

Author Manuscript

Author Manuscript

Author Manuscript

Author Manuscript

**Figure 8.**

The expression of lipid biosynthesis genes is reduced in the mammary glands of AFAP1^{-/-} mice during early lactation. **A.** Tissue lysates were prepared from the mammary glands from AFAP1^{+/+} and AFAP1^{-/-} mice at late pregnancy (P16.5) and early lactation (L3). The expression levels of SREBP1, ACC1 and FAS were determined by western blot. β-actin was used as a loading control. **B.** Cryosections of mammary glands at early lactation (L3) were prepared from AFAP1^{+/+} (a, c) and AFAP1^{-/-} (b, d) mice and stained with Oil Red O and counterstained with hematoxylin. Images at both low magnification (a and b, bars = 200 μm) and high magnification (c and d, bars = 20 μm) are shown.

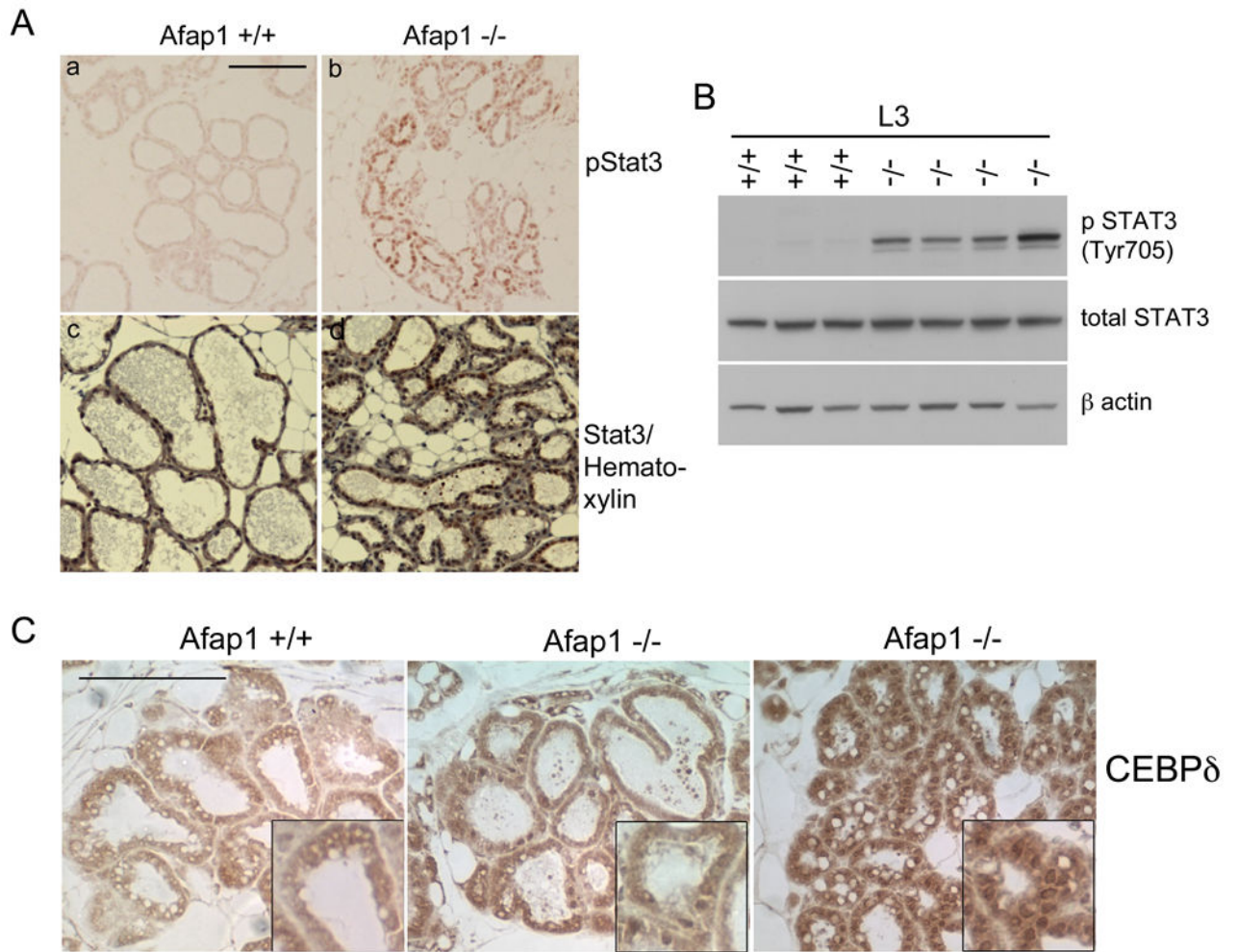


Figure 9.

Enhanced Stat3 tyrosine phosphorylation and CEBPδ nuclear localization in AFAP1^{-/-} mammary glands are molecular indicators of precocious involution. **A.** Histological sections of mammary glands at early lactation (L3) were prepared from AFAP1^{+/+} (a, c) and AFAP1^{-/-} (c,d) mice and stained for phosphoSTAT3 (a,b) and total STAT3 together with hematoxylin counterstaining (c,d). Bars = 100 μm. **B.** Western blot analysis of phospho-STAT3 and total STAT3 in tissue lysates prepared from the mammary glands of AFAP1^{+/+} and AFAP1^{-/-} mice at L3. β-actin was used as a loading control. **C.** Histological sections as in panel A were stained for CEBPδ (two mammary glands at L3 from AFAP1^{-/-} mice are shown). Note the enhanced nuclear localization of CEBPδ in the enlarged images (boxes) of the mammary glands from AFAP1^{-/-} mice at L3.